The Jag2/Notch1 signaling axis promotes sebaceous gland differentiation and controls progenitor proliferation

Syeda Nayab Fatima Abidi[1*], Sara Chan[2], Kerstin Seidel[1], Daniel Lafkas[1], Louis Vermeulen[1], Frank Peale[2], and Christian W. Siebel[1*]

[1] Department of Discovery Oncology, Genentech, South San Francisco, CA, USA

[2] Department of Research Pathology, Genentech, South San Francisco, CA, USA

* Co-corresponding authors

Abstract

The sebaceous gland (SG) is a vital appendage of the epidermis, and its normal homeostasis and function is crucial for effective maintenance of the skin barrier. Notch signaling is a well-known regulator of epidermal differentiation, and has also been shown to be involved in postnatal maintenance of SGs. However, the precise role of Notch signaling in regulating SG differentiation in the adult homeostatic skin remains unclear. While there is evidence to suggest that Notch1 is the primary Notch receptor involved in regulating the differentiation process, the ligand remains unknown. Using monoclonal therapeutic antibodies designed to specifically inhibit of each of the Notch ligands or receptors, we have identified the Jag2/Notch1 signaling axis as the primary regulator of sebocyte differentiation in homeostatic skin. Mature sebocytes are lost upon specific inhibition of the Jag2 ligand or Notch1 receptor, resulting in the accumulation of proliferative stem/progenitor cells in the SG. Strikingly, this phenotype is reversible, as these stem/progenitor cells re-enter differentiation when the inhibition of Notch activity is lifted. Thus, Notch activity promotes correct sebocyte differentiation, and is required to restrict progenitor proliferation.

Introduction

The skin is a vital organ that acts as a protective barrier against the external environment, and safeguards against fluid loss. An important component of this barrier function is the presence of a complex mixture of oils, known as sebum, which is produced by the sebaceous glands (SGs). SGs are part of the epidermis and are typically associated with the hair follicle. These acinar structures have two cell types:

basal stem or progenitor cells which encase the differentiated sebocytes (Figure 1a). Sebocyte differentiation begins at the proximal tip of the of the SG, with maturing sebocytes moving upwards, enlarging, accumulating lipids, and ultimately undergoing a highly regulated and specialized form of cell death in which they release their lipid contents into the sebaceous duct (Figure 1b) (Kretzschmar et al., 2014; Schneider and Paus, 2010). This process requires the constant turnover of sebocytes, which occurs over a period of 7-14 days in mice (Jung et al., 2015). Both over- and underproduction of sebum have been linked to various skin disorders including acne or dry skin (Al-Zaid et al., 2011; Binczek et al., 2007; Karnik et al., 2009; Lovászi et al., 2017; Rittié et al., 2016; Seiffert et al., 2007; Shi et al., 2015; Smith and Thiboutot, 2008; Stenn et al., 1999), and rare sebaceous carcinomas constitute aggressive tumors leading to high mortality (Buitrago and Joseph, 2008; Nelson et al., 1995), thus SG number and function have to be tightly regulated for proper skin function.

The Notch signaling pathway is one of the most studied regulators of cell fate decisions, and is known to be widely involved in epidermal differentiation. The pathway consists of multiple ligands and receptors that typically form a signaling axis in pairs. Notch signaling can regulate cell fate by either inducing or inhibiting differentiation, or by making binary cell fate decisions (Wilson and Radtke, 2006). Classically, these functions of Notch signaling have been studied during development, but increasing evidence suggests that the Notch pathway is also involved in regulating cell fate and cell states in adult homeostatic tissues (Ables et al., 2011; Lafkas et al., 2015; Mosteiro et al., 2023; Sato et al., 2012; Siebel and Lendahl, 2017).

While it is known that Notch signaling is not required for embryonic development of the epidermis, it is essential for the postnatal maintenance of the hair follicles and the SGs (Watt et al., 2008). However, the precise role of Notch signaling in adult sebocyte differentiation has not been comprehensively investigated, with most studies examining irreversible deletions of the Notch pathway components in the embryonic ectodermal lineages. While these studies report SG defects, it remains unclear whether these defects are due to a direct effect on the SGs, or whether they are a consequence of general skin defects also observed in these models. For example, SGs are absent in mice with embryonic pan-Notch deletions such as *RBPJ* (Blanpain et al., 2006), gamma-secretase, *Notch1Notch2*, and *Notch1Notch2Notch3*, and are severely reduced in *Notch1* and *Notch1Notch3* embryonically-deleted skin (Pan et al., 2004), while deletion of *Notch2* alone does not affect the SG (Pan et al., 2004). Consistent with the constitutive deletions, loss of *RBPJ* in adult SGs also results in missing sebocytes, while loss of *Notch1* in the adult SGs results in miniaturized lobes that still contain some differentiated sebocytes (Veniaminova et al., 2019). Interestingly, activation of *Notch1* in the adult skin results in enlarged SGs (Estrach et al., 2006). Conversely, for the Notch pathway ligands, embryonic and adult deletion of *Jag1* (Estrach et al., 2006), and embryonic deletion of *Dll1*(Estrach et al., 2008) results in normal SG morphology. Collectively, these data suggest that Notch1 is the dominant Notch receptor involved in regulating sebocyte differentiation, however, it remains unclear which ligand is required.

In our previous work, we observed that systemic inhibition of Jag2 using monoclonal therapeutic antibodies resulted in SG defects in adult mice (Lafkas et al., 2015). Given that our therapeutic antibodies selectively, potently, and transiently inhibit each of the distinct Notch receptors and ligands (Tran et al., 2013; Wu et al., 2010; Yu et al., 2020), they constitute ideal tools to dissect the contribution of each of these pathway members to sebocyte differentiation in adult homeostatic skin. Leveraging the use of these antibodies, we demonstrate that specific inhibition of the Jag2 ligand or Notch1 receptor both result in the loss of mature sebocytes in the SG, establishing the Jag2/Notch1 signaling axis as a crucial regulator of sebocyte differentiation in adult homeostatic skin. The loss of mature sebocytes in the SG is concomitant with an accumulation of cells with a basal phenotype, forming epithelial remnants in the SG. Cells in these epithelial remnants are actively proliferating and express stem/progenitor markers indicating that sebocyte differentiation is halted, while stem/progenitor numbers are increased. Importantly, this phenotype is reversible, as these epithelial cells re-enter differentiation with the return of Notch activity. Thus, Notch activity is required in sebocyte stem/progenitor cells for their proper differentiation, and its inhibition locks these cells in a reversible progenitor state.

Results

Jag2 is the dominant Notch signaling ligand involved in regulating sebocyte differentiation

To investigate the role of Notch signaling in the homeostatic skin, we treated 8-week old mice with a single dose of the various antagonizing antibodies (anti-Notch1, anti-

Notch2, anti-Jag1, anti-Jag2 and the isotype control antibody anti-Ragweed) alone or in combination. We then examined the dorsal, resting phase (telogen) skin at 3, 7 and 14 days post treatment. We first confirmed that our antibodies could reproduce the requirement of Notch1 in regulating sebocyte differentiation. To this end, we treated mice with Notch1 (aN1) and Notch2 (aN2) blocking antibodies and examined the SGs at 7 days post treatment. Loss of mature sebocytes was observed specifically after aN1 treatment, while the aN2 treated SGs showed normal morphology (Figure 1c,d). However, the combined treatment of aN1N2 had a more pronounced effect on SG morphology as compared to aN1 alone (Figure 1c,d), indicating that Notch2 also contributes to regulating sebocyte differentiation, possibly as a compensatory mechanism after inhibition of the dominant Notch1 receptor.

Next, we investigated which ligand formed the signaling pair with Notch1. Loss of mature sebocytes was observed specifically after treatment with the Jag2 blocking antibody (aJ2), but not after treatment with the Jag1 blocking antibody (aJ1) at 7 days post treatment (Figure 1e,f). For aJ2 treatment, the loss of sebocytes began at 3 days post treatment, but affected only a small proportion of the SGs at this timepoint (Figure 1g). However, by 7 days post treatment, most SGs had either completely lost all sebocytes, or had only some sebocytes remaining (Figure 1g). The loss-of-sebocyte phenotype was most pronounced with a combined treatment of Jag1/Jag2 blocking antibodies (aJ1J2) (Figure 1g), suggesting that while Jag2 is the primary Notch ligand involved in regulating sebocyte differentiation, Jag1 also plays a minor role in this process, but is unable to produce a phenotype on its own. In conclusion, these data

indicate that the Jag2-Notch1 signaling axis is the dominant Notch ligand-receptor pair required for sebocyte differentiation in the adult skin.

We also examined the percentage of SGs consisting of bursting sebocytes releasing sebum as a proxy of a functional sebaceous duct. There were no significant differences between treatments (Figure S1a,b), hinting at a functionally intact sebaceous duct.

Notch is active in the sebaceous gland stem cells

We next characterized the expression of the relevant receptor and ligand in the SG to develop a spatial map of Notch activity in this tissue. Both the Notch receptors and their ligands are transmembrane proteins that interact with each other on neighboring cells to activate the pathway. To examine this interaction, we performed a triple stain for the cleaved (active) form of the Notch1 intracellular domain (ICD), and Notch1 and Jag2 in situ hybridization (ISH) probes at 3 days post antibody treatment. In the control treated mice, Notch1 ICD was observed in the basal stem cell compartment of the SG, but not in the differentiating sebocytes (Figure 2a-c, cell types based on morphology). We saw a similar pattern of N1ICD-postive cells for aJ1 treatment (Figure 2d-f). Notch1 signaling was not active in all basal cells, as only ~50% of them were positive for N1ICD after control and aJ1 treatment (Figure 2g). Consistent with previous studies, the majority of these N1ICD+ cells were present near the proximal tip of the SG (Figure S2a-c) (Veniaminova et al., 2019), where the initial sebocyte differentiation has been proposed to occur (Kretzschmar et al., 2014). However, after aJ2 treatment, Notch1 activity (ICD staining) was absent, or observed only at very low levels in the basal stem cells, while

they still expressed Notch1 and Jag2 mRNA (Figure 2h-j). Strikingly, we noticed the expression of both Notch1 ISH and Jag2 ISH in the same cell on most N1ICD+ cells (Figure 2k). Interestingly, a majority of all basal cells (including N1ICD- cells), expressed both N1 and Jag2 mRNA (Figure S2d). Our data shows that the vast majority of SG basal stem cells express both the ligand and receptor, but only some basal stem cells experience active Notch signaling at any one point in time, as evidenced by the presence of N1ICD. This could be a technical limitation as the triple staining only captures a temporal snapshot of the basal stem cells, with the N1+J2 mRNA positive cells going on to express N1ICD later, or it could hint towards a more complex regulatory mechanism involved in activating Notch signaling.

Notch activity, as well as Notch1 and Jag2 mRNA were also observed in the interfollicular epidermis (IFE) and other cells of the hair follicle (Figure S2e,f). While there is a reduction in Notch-active cells in these other regions, it does not appear to significantly impact the rest of the skin. There were no significant differences in the width of the IFE or the adipocyte layer between treatments (Figure S2g,h). This together with the histological appearance (FigureS2i,j) of these regions suggests that proliferation and differentiation in these compartments remains unaffected.

Loss of Notch activity in the SG stem cells inhibits sebocyte differentiation

To further detail the effect of Notch inhibition on sebocyte differentiation, we examined the expression of mature sebocyte markers. Adipophilin (Adipo) is expressed in all mature sebocytes (Frances and Niemann, 2012; Ostler et al., 2010) and Fatty acid

synthase (FASN) is expressed in mid- and late-differentiating sebocytes, with FASN levels decreasing in the most mature sebocytes (Cottle et al., 2013) (Figure 1b). Since N1ICD staining disappears at 3 days post antibody treatment, we examined the mature sebocyte markers at this timepoint. While N1ICD staining was specifically lost in the SG basal stem cells of aJ2 treated skin, mature sebocytes expressing FASN were still observed at this timepoint (Figure 2j, Figure 3a,b and Figure S3a). All cells that express FASN also express adipophilin, but since FASN levels decrease with sebocyte maturity, we also examined and focused on adipophilin to mark all sebocytes (Figure 3c,d and Figure S3b-e). The number of cells that expressed adipophillin were not significantly different between treatments at 3 days post antibody treatment (Figure 3h). At 7 days post antibody treatment, control and aJ1 treated skin showed normal SG morphology and sebocyte marker expression (Figure 3e and Figure S3f,h,i), but both aJ2 and aJ1J2 SGs had lost sebocyte marker expression, and the SG was filled with cells with a basal phenotype (basal-like cells) (Figure 3f and Figure S3g,j,k). Consistently, the number of cells expressing adipophilin were significantly lower for aJ2 and aJ1J2 treatment (Figure 3i). Interestingly, we noticed that some of these affected SGs still contained a few mature sebocytes (Figure 3f and Figure S3g), which were found at the distal end near the sebaceous duct. The location of these remaining sebocytes suggests that existing mature sebocytes are not affected by the Notch blockade, and go through their normal differentiation process, eventually bursting and releasing the sebum (Figure 3g). Thus, we propose that Notch blockade inhibits differentiation at basal stem cell-level or in a sebocyte progenitor.

Notch activity in the SG stem cells is required to prevent unregulated progenitor proliferation

To determine whether the epithelial cells that filled the affected SGs at 7 days post treatment were stem/progenitor cells, we examined them for stem and early differentiation markers. Lrig1 positive cells form a distinct stem cell compartment that maintains the SG and the upper part of the hair follicle (Frances and Niemann, 2012; Niemann and Horsley, 2012; Page et al., 2013), allowing us to use Lrig1 as a marker for the basal stem cells of the SG, while Androgen Receptor (AR) can be used as an early marker of sebocyte differentiation (Cottle et al., 2013) (Figure 4a,b and Figure S4a,b). We noticed that the AR-expressing cell population could be divided into two groups: a basal stem cell population that co-expressed Lrig1, but did not express FASN (arrow heads in Figure 4a,c), and an early differentiating sebocyte population that expressed FASN, but did not express Lrig1 (arrows in Figure 4a,c). We hypothesize that the Lrig1+/AR+ population is a progenitor cell population, in addition to the Lrig1+ stem cells, similar to the recently identified transitional basal cell population in the SG (Veniaminova et al., 2023). There were no significant differences in the number of Lrig1 positive stem cells per SG, or the AR-expressing progenitor population between treatments at 3 days post treatment (Figure 4d,e). By 7 days post treatment, however, the basal-like cells that filled the SG were all positive for Lrig1 (Figure 4f,g and Figure S4e), with the total number of Lrig1 positive cells per SG increasing significantly for aJ2 and aJ1J2 treated SGs (Figure 4h), while SGs after aJ1 treatment showed normal morphology and marker expression (Figure S4c,d). The proportion of AR-expressing cells was not significantly different between treatments (Figure 4i). These results

indicate that the basal-like cells that fill the SG after blocking Notch signaling by aJ2 and aJ1J2 treatment, are stem/progenitor cells. Additionally, we examined the SGs for their proliferative capacity to confirm stem/progenitor function. In a normal SG, proliferation is restricted to the basal stem cells (Figure 4j). As expected, proliferation was also restricted to the basal stem cells in aJ1 treated SGs (Figure S4f,g). Remarkably, most of the basal-like cells in the aJ2 treated SGs were proliferative, while the rare mature sebocytes remaining in the SG were non-cycling (Figure 4k). As the SGs are mostly filled with basal-like cells at this time (Figure 4h), the total number of proliferating cells per SG was significantly higher (Figure 4l).

Overall, these data suggest that inhibition of Notch activity by aJ2 treatment retains the stem and progenitor (Lrig1+ and Lrig1+/AR+, respectively) cells in their immature proliferative state and prevents differentiation.

The block in sebocyte differentiation is lifted upon recovery of Notch activity

The therapeutic antibodies employed do not inhibit Notch signaling permanently, as the antibodies eventually become cleared from the animal's system. To determine whether the loss of sebocyte phenotype was reversible, we examined the SGs 14 days post single-dose treatment. Intriguingly, mature sebocytes begin to recover at this time point (Figure 5a,b, compare with Figure 1f,g). We hypothesized that the sebocyte recovery must be due to the return of Notch activity after antibody washout. To test this, we examined the SGs for Notch activity at 7 days post treatment, since the return of Notch activity must precede the recovery of mature sebocytes. Fittingly, we observed N1ICD

expression return in some of the basal-like cells at this time (Figure 5c,d and Figure S5a-d). The percent of N1ICD positive cells per SG strongly increased from 1% at 3 days post treatment to 29% at 7 days post treatment (Figure 5e), even though the percentage of N1ICD positive cells per SG remained significantly lower than control for aJ2 and aJ1J2 treated SGs at this time (Figure S5d). Next, we examined the SGs at 14 days post treatment for mature sebocyte markers to confirm the sebocyte recovery. Indeed, we saw the return of cells expressing adipophilin in the aJ2 and aJ1J2 treated SGs (Figure 5f,g and Figure S5e-h). There was an overall increase in the number of these cells from day 7 to day 14 (Figure 5h), even though the number of these cells remained significantly lower in these SGs compared to controls (Figure S5h). Interestingly, the majority of the adipophilin expressing cells were found in the proximal third of the SG (51% for aJ2 treatment and 66% for aJ1J2 treatment), consistent with the initiation of sebocyte differentiation at the proximal tip. However, there was a significant proportion of these cells found in the middle third (22% and 25% respectively), and distal third (27% and 9% respectively) of the SG. This could be due to the newly differentiated cells moving through the SG in a proximal to distal direction, as is the case during normal homeostasis. Alternatively, the stem cells could also be differentiating at sites other than just the proximal tip, as previously demonstrated by multi-color lineage tracing (Andersen et al., 2019). We further examined the SGs at 14 days post treatment for their AR expression, and confirmed that it had also been restored to its normal pattern (Figure 5i,j and Figure S5i-l). We also found that the average number of AR-expressing cells decreased from day 7 to day 14 post aJ2 and aJ1J2 treatment (10 to 2.95, and 8.56 to 5.55, respectively) (Figure 5k), returning to a

more homeostatic state. Together, these data indicate that Notch inhibition does not result in a permanent cell fate switch, but maintains the stem/progenitor state, allowing the recovery of the differentiation process with the restoration of Notch activity.

Discussion

Based on our findings, we propose that the Jag2/Notch1 signaling axis is essential for correct sebocyte differentiation in homeostatic dorsal skin, and that inhibition of this signaling retains the basal stem and progenitor cells in a proliferative state, and blocks further differentiation. Thus, Notch signaling is required to prevent unregulated stem/progenitor proliferation, and induction of the sebocyte differentiation program. Moreover, Notch inhibition resulting in complete loss of mature sebocyte differentiation is a reversible phenotype, indicating that there remains a functional progenitor pool present during the studied timeframe.

Here, we have leveraged the use of monoclonal therapeutic antibodies designed to inhibit each of the distinct Notch receptors or ligands to study the role of Notch signaling in adult homeostatic tissue. We have shown that Jag2 is the hitherto unknown ligand involved in regulating sebocyte differentiation. Inhibition of Notch signaling using Jag2 blocking antibodies results in the loss of mature sebocytes, with the resulting SG being filled with basal-like cells forming “finger-like” epithelial remnants. A similar phenotype has been described by a previous study (Veniaminova et al., 2019) that used Lrig1-CreERT2 to irreversibly knock out RBPJ in adult homeostatic skin. This strategy enabled inhibition of Notch signaling specifically in the Lrig1+ stem cell population that

normally maintains the SGs, but preserved it in the rest of the hair follicle. Interestingly, the authors saw two contradictory phenotypes as a result: overall loss of SG lobes, replaced by the finger-like epithelial remnants, as well as the presence of persistent SGs that were enlarged. The authors showed that over time, patches of Rbpj mutant cells extended out of their niche into the interfollicular epidermis (IFE), where Lrig1 is not expressed, and that loss of RBPJ in the IFE led to enlarged SGs. They argue that while Notch signaling promotes sebocyte differentiation in the SG stem cells, it indirectly suppresses these glands from the IFE. Our results did not show the enlarged SG phenotype, and we only observed the finger-like epithelial remnants. While injections of the Notch blocking antibodies are systemic, we only observed a reduction in the number of Notch-active cells in the IFE, but not a complete loss. This could explain why we didn't observe the enlarged SG phenotype. Additionally, we observed the phenotype as early as 3 days post antibody treatment, while Veniaminova et al., observed the SGs 10 weeks after tamoxifen injection. These differences are likely due the different methodologies used in the two studies.

Several studies indicate that Notch signaling is essential for the postnatal maintenance of SGs (Blanpain et al., 2006; Estrach et al., 2008, 2006; Pan et al., 2004; Watt et al., 2008), but so far only Veniaminova et al., have specifically examined SGs in the adult homeostatic skin. They observed that the stem/progenitor and differentiation markers were intermingled in the finger-like remnants forming an unnatural hybrid state, neither staying in a true progenitor state nor differentiating. In contrast, we observed a complete block in differentiation, with the stem/progenitor cells being locked in an immature

proliferative state. These observations suggest that antagonistic antibodies may be able to achieve a more complete inhibition of Notch signaling in the SG stem/progenitor compartment.

Importantly, we were able to show that the loss-of-sebocyte phenotype in the SG is reversible. Having used therapeutic antibodies to block Notch signaling, the inhibition of the signaling pathway was not permanent. As Notch activity returned to the SG after antibody washout, sebocyte differentiation also recovered. These data indicate that the loss of Notch signaling does not impact the stem/progenitor potential of the SG, but prevents further differentiation. Indeed, a functional progenitor pool accumulates in the SG, primed for differentiation, as soon as Notch signaling becomes active. A recent study by Veniaminova et al., has shown that Lrig1-CreERT2 used to irreversibly knock out *Pparg* in adult homeostatic skin ablates 99% of the SGs (Veniaminova et al., 2023). Interestingly, they showed that non-recombined cells from other parts of the hair follicle migrate to the SG zone and regenerate the genetically ablated SGs. This regeneration process is dependent on the hair growth cycle, with the SGs primarily regenerating during anagen (active growth) phase and not in the telogen phase. While our studies cannot rule out the contribution of non-SG cells to the SG recovery seen upon return of Notch activity, this recovery is not dependent on the hair growth cycle. Sebocytes are able to differentiate while the hair follicle is still in the telogen phase, indicating a lift of the differentiation block on the stem/progenitor cells. This reversibility of phenotype is intriguing from a therapeutic perspective, as it suggests a translational potential in skin disorders involving sebocyte overactivity, such as acne.

An important open question is how Notch signaling regulates sebocyte differentiation. FASN, which can be used as a readout for sebocyte differentiation, is a downstream target of AR (Schirra et al., 2005). We observed an Lrig1+/AR+/FASN- population in the normal SGs, similar to the basal-like cells that fill the finger-like remnants seen after Notch inhibition. This expression pattern indicates that AR requires a co-activator to activate downstream gene expression in the SG. Previous studies have reported that Notch effectors such as HEY1, HEY2 and HEYL can act as co-repressors of AR in prostate cells (Belandia et al., 2005; Kamińska et al., 2020; Lavery et al., 2011). It is possible that certain Notch effectors can act as either co-activators or co-repressors of AR in a context-dependent manner. Further investigation will be needed to understand the exact molecular role Notch signaling plays in regulating sebocyte differentiation.

Methods

Animal strains and treatments

All animal experimentation was performed according to protocols approved by the Genentech Institutional Animal Care and Use Program (IACUC) committee. Female C57BL/6 mice were obtained from Charles River-Hollister, and were used for all experiments. The mice were 8 weeks old upon treatment. This time point was chosen to correspond to the resting (telogen) phase of the hair growth cycle, as SG size can vary by hair cycle stage. All mice were injected intraperitonially with a single dose of blocking antibodies diluted in sterile saline at the following concentrations: anti-Jag1 at 20mg/kg, anti-Jag2 at 20mg/kg, anti-Jag1+anti-Jag2 at 20mg/kg+20mg/kg = 40mg/kg, anti-Notch1

at 5mg/kg, anti-Notch2 at 10mg/kg and anti-Notch1+anti-Notch2 at 5mg/kg+10mg/kg = 15mg/kg. Anti-Ragweed isotype control antibody was injected at concentrations to match the maximum dose of treatment antibodies.

Histopathological analysis and immunochemistry

Telogen mouse dorsal skin was collected at 3, 7 and 14 days post antibody injection. For frozen sections, skin samples were fixed in 4% paraformaldehyde in PBS, for 40 minutes at 4°C, washed, and then immersed in 30% sucrose in PBS overnight at 4°C. The tissue was then embedded in OCT (TissueTek), frozen immediately on dry ice, and stored at -80°C. Additional skin tissue from the same animals was also fixed with 10% neutral buffered formalin and then used to create paraffin-embedded sections. Hematoxylin and eosin (H&E) staining was performed by the Pathology core at Genentech.

The triple immunofluorescence stain for Notch1 ICD (IHC), and Notch1 mRNA (ISH) and Jag2 mRNA (ISH) was performed by the histopathology development group at Genentech. ACD LS 2.5 probes were ordered from Advanced Cell Diagnostics. RNAScope LS 2.5 Murine-Jag2_C1 (417518) nucleotides spanning from nt 552-1480 of reference sequence NM_010588.2, and Murine-Notch1_C2 (404648-C2) nucleotides spanning from nt 1153-1960 of reference sequence NM_008714.3. For positive control RNAScope LS 2.0 Murine-PPIB probe (313917) nucleotides spanning from nt 98~856 of reference sequence NM_011149.2 were used. For negative control RNAScope LS 2.0 DapB probe (312038) nucleotides spanning from nt 414~862 reference sequence

EF191515 were used. For Immunohistochemistry, we used N1ICD (Cell Signaling, 4147), at 20 ug/ml working concentration.

The triple immunofluorescence for murine Jag2_Notch1 (dual ISH) with anti_Notch1 ICD (IHC) 3 Plex ISH_ISH_IHC in murine tissues using formalin-fixed, paraffin-embedded sections was performed on the Leica Bond-RX complete automation system using the RNAscope® LS Multiplex Reagent Kit (322800). Slides were baked and dewaxed on Leica Bond-RX and pretreated with Bond Epitope Retrieval Solution 2 (ER2) (AR9640) from Leica at 100°C for 40 minutes. After pretreatment, the probes were cocktailed, and hybridization was performed at 42°C for 120 minutes followed by amplification steps and developed with Opal 570 fluor at 1:1000 and Opal 690 fluor at 1:1500 from Akoya using the Opal Polaris 7 Auto Detection Kit (NEL811001KT). The immunohistochemistry was performed upon completion of ISH. The primary antibody incubation was 60 minutes at room temperature, followed by secondary antibody incubation for 30 min at room temperature with HRP conjugated Goat anti Rabbit (Perkin Elmer, NEF812001EA). The slides were then developed with Opal 780 fluor at 1:25 (Akoya, SKU FP1501001KT) following the manufacturer's instructions. Slides were imaged using Olympus VS200.

All other immunohistochemistry was performed using the following antibodies: N1ICD at 1:500 (Cell Signaling, 4147), FASN at 1:100 (BD, 610963), Adipophillin at 1:500 (Fitzgerald, 20R-AP002), Ki67 at 1:100 (Thermo Fisher Scientific, SP6 RM-9106-SO),

Lrig1 at 1:200 (R&D Systems AF3688-SP), and AR at 1:250 (Thermo Fisher Scientific, MA1-150 AN1-15). Slides were imaged using the Leica Thunder microscope.

Imaging parameters were identical for all images. Images were processed using Fiji and Adobe Illustrator.

Acknowledgements

We are grateful to C. Cottonham, S. Hankeova, G. Hernandez for helpful discussions. We thank the Genentech Research Pathology, Necropsy, and Histology laboratories for their experimental contributions. We appreciate the insightful feedback and comments on the paper from L. Mosteiro, E. Reyes and B. Biehs.

Author contributions

S.N.F.A. designed the project, performed experiments and data analysis, and wrote the manuscript. S.C. developed the triple stain methodology, and performed the relevant staining. K.S. helped with some experimental design. The first observation of the phenotype came out of D.F.'s work. L.V. analyzed the data and contributed to writing the manuscript. F.P. provided histopathological analysis and discussion. C.W.S. directed and supervised the research, and analyzed the data. All authors approve the content of the manuscript.

Conflict of interest

All authors are or where employees of Genentech Inc. and/or hold shares in Roche. C.W.S is currently employed at Gilead Sciences.

Figure Legends

Figure 1. Jag2 is the dominant ligand involved in regulating sebocyte differentiation.

(a) A representative image of the homeostatic hair follicle, including its associated sebaceous gland (SG). (b) A detailed schematic of the SG showing the outer basal stem cell layer encasing the differentiated sebocytes. The schematic also shows the gene expression in different regions of the SG. (c) Representative H&E images of SGs from mice (n = 5 each) treated with aRW, aN1, aN2 and aN1N2, 7 days post treatment. (d) Quantification of type of SG found after each treatment. The SGs were divided into three categories: normal SGs containing characteristic number of sebocytes (normal SG), SGs containing a mix of sebocytes and basal-like cells (mixed SG), and SGs containing no sebocytes and only basal-like cells (no sebocyte SG). For (c), (e) and (f), each SG panel is labeled with where the SG is normal, mixed or no sebocyte SG. p-values: aN1 = 2.02E-123, aN2 = 0.426, aN1N2 = 3.85E-114. Total n of SGs quantified per treatment: aRW = 425, aN1 = 298, aN2 = 343, aN1N2 = 217. (e) Representative H&E images of SGs from mice (n = 5 each) treated with aRW, aJ1 and aJ2, 3 days post treatment. (f) Representative H&E images of SGs from mice (n = 5 each) treated with aRW, aJ1, aJ2 and aJ1J2, 7 days post treatment. (g) Quantification of type of SG found after each treatment. 3 days: p-values: aJ1 = 0.409, aJ2 = 0.004. 7 days: p-values: aJ1 = 0.057, aJ2 = 7.61E-151, aJ1J2 = 6.23E-169. Total n of SGs quantified per treatment:

3 days, aRW = 851, aJ1 = 944, aJ2 = 760, 7 days, aRW = 491, aJ1 = 499, aJ2 = 388, aJ1J2 = 461. Chi-sqaure test used for statistical analysis. All treatments compared against aRW. Error bars represent SEM. Scale bars are 100 μm.

Figure 2. Notch is active in the sebaceous gland stem cells.

(a-c) Representative triple stain images for N1ICD, Notch1 and Jag2 mRNA in SGs from mice (n = 5 each) treated with aRW, 3 days post treatment. (a) Four channels showing N1ICD, N1 ISH, J2 ISH and DAPI. (b) Two channels showing N1 ISH and J2 ISH. (c) One channel showing N1ICD. (d-f) Representative triple stain images for N1ICD, Notch1 and Jag2 mRNA in SGs from mice (n = 5 each) treated with aJ1, 3 days post treatment. (d) Four channels showing N1ICD, N1 ISH, J2 ISH and DAPI. (e) Two channels showing N1 ISH and J2 ISH. (f) One channel showing N1ICD. (g) Quantification of the percentage of N1ICD positive (N1ICD+) basal stem cells in SGs from mice (n = 5 each) treated with aRW, aJ1 and aJ2, 3 days post treatment. Percentage was calculated by dividing the number N1ICD+ basal stem cells by total number of basal stem cells in each SG. (h-j) Representative triple stain images for N1ICD, Notch1 and Jag2 mRNA in SGs from mice (n = 5 each) treated with aJ2, 3 days post treatment. (h) Four channels showing N1ICD, N1 ISH, J2 ISH and DAPI. (i) Two channels showing N1 ISH and J2 ISH. (j) One channel showing N1ICD. (k) Quantification of what percentage of the N1ICD+ basal stem cells express both N1 ISH and J2 ISH, only N1 ISH or only J2 ISH. (g and k) Total n of SGs quantified per treatment: aRW = 13, aJ1 = 15, aJ2 = 15. Error bars represent SEM. Scale bars are 25 μm.

Figure 3. Loss of Notch activity in the SG stem cells inhibits sebocyte differentiation.

(a,b) Representative co-stain images for N1ICD and FASN in SGs from mice (n = 5 each) treated with aRW (a) and aJ2 (b), 3 days post treatment. (c,d) Representative adipophillin staining in SGs from mice (n = 5 each) treated with aRW (c) and aJ2 (d), 3 days post treatment. (e,f) Representative adipophillin staining in SGs from mice (n = 5 each) treated with aRW (e) and aJ2 (f), 7 days post treatment. (g) A representative H&E image of an SG from mice (n = 5 each) treated with aJ2, 7 days post treatment. Arrow points to a bursting sebocyte releasing sebum into the sebaceous duct. (h) Quantification of the number of cells expressing adipophilin in each SG, 3 days post treatment with aRW, aJ1 and aJ2. p-values: aJ1 = 0.749, aJ2 = 0.062. Total n of SGs quantified per treatment: aRW = 17, aJ1 = 14, aJ2 = 30. (i) Quantification of the number of cells expressing adipophilin in each SG, 7 days post treatment with aRW, aJ1, aJ2 and aJ1J2. p-values: aJ1 = 0.301, aJ2 = 4.13E-14, aJ1J2 = 4.06E-14. Total n of SGs quantified per treatment: aRW = 18, aJ1 = 19, aJ2 = 22, aJ1J2 = 21. Student's T-test used for statistical analysis. All treatments compared against aRW. Error bars represent SEM. Scale bars are 25 μm.

Figure 4. Notch activity in the SG stem cells is required to prevent unregulated progenitor proliferation.

(a,b) Representative co-stain images for Lrig1 and AR in SGs from mice (n = 5 each) treated with aRW (a) and aJ2 (b), 3 days post treatment. (c) A representative co-stain

image for FASN and AR in an SG from mice (n = 5 each) treated with aRW, 3 days post treatment. Arrows point to sebocytes, and arrowheads point to progenitor cells. (d) Quantification of the number of cells expressing Lrig1 in each SG, 3 days post treatment with aRW, aJ1 and aJ2. p-values: aJ1 = 0.152, aJ2 = 0.450. (e) Quantification of what percentage of the Lrig1+ cells express AR, 3 days post treatment with aRW, aJ1 and aJ2. p-values: aJ1 = 0.789, aJ2 = 0.028. (d and e) Total n of SGs quantified per treatment: aRW = 17, aJ1 = 10, aJ2 = 24. (f,g) Representative co-stain images for Lrig1 and AR in SGs from mice (n = 5 each) treated with aRW (f) and aJ2 (g), 7 days post treatment. (h) Quantification of the number of cells expressing Lrig1 in each SG, 7 days after treatment with aRW, aJ1, aJ2 and aJ1J2. p-values: aJ1 = 0.628, aJ2 = 9.06E-07, aJ1J2 = 7.88E-06. (i) Quantification of what percentage of the Lrig1+ cells express AR, 7 days after treatment with aRW, aJ1, aJ2 and aJ1J2. p-values: aJ1 = 0.117, aJ2 = 0.248, aJ1J2 = 0.091. (h and i) Total n of SGs quantified per treatment: aRW = 12, aJ1 = 12, aJ2 = 18, aJ1J2 = 16. (j,k) Representative co-stain images for Ki67 and FASN in SGs from mice (n = 5 each) treated with aRW (j) and aJ2 (k), 7 days post treatment. (l) Quantification of the number of cells expressing Ki67 in each SG, 7 days after treatment with aRW, aJ1, and aJ2. p-values: aJ1 = 0.652, aJ2 = 0.009. Total n of SGs quantified per treatment: aRW = 11, aJ1 = 12, aJ2 = 16. Student's T-test used for statistical analysis. All treatments compared against aRW. Error bars represent SEM. Scale bars are 25 μm.

Figure 5. The block in sebocyte differentiation is lifted upon recovery of Notch activity.

(a) Representative H&E images of SGs from mice (n = 5 each) treated with aRW, aJ1, aJ2 and aJ1J2, 14 days post treatment. (b) Quantification of type of SG found after each treatment. The SGs were divided into three categories: normal SGs containing characteristic number of sebocytes (normal SG), SGs containing a mix of sebocytes and basal-like cells (mixed SG), and SGs containing no sebocytes and only basal-like cells (no sebocyte SG). p-values: aJ1 = 0.535, aJ2 = 2.90E-87, aJ1J2 = 1.73E-92. Chi-sqaure test used for statistical analysis. All treatments compared against aRW. Total n of SGs quantified per treatment: aRW = 485, aJ1 = 430, aJ2 = 394, aJ1J2 = 364. Scale bars are 100 µm. (c,d) Representative co-stain images for N1ICD and FASN in SGs from mice (n = 5 each) treated with aRW (c) and aJ2 (d), 7 days post treatment. (e) Quantification of the percentage of N1ICD+ cells in SGs from mice (n = 5 each) treated with aRW and aJ2, 3 and 7 days post treatment. Percentage was calculated by dividing the number N1ICD+ cells by total number of basal-like cells in each SG. p-values: for comparison between day 3 and day 7 for aRW treatment = 0.297, for comparison between day 3 and day 7 for aJ2 treatment = 1.00E-14. Total n of SGs quantified per treatment: aRW at 3days = 13, aRW at 7days = 13, aJ2 at 3days = 15, aJ2 at 7 days = 22. (f,g) Representative adipophillin staining in SGs from mice (n = 5 each) treated with aRW (f) and aJ2 (g), 14 days post treatment. (h) Quantification of the number of cells expressing adipophilin in each SG, 7 and 14 days after treatment with aRW, and aJ2. p-values: for comparison between day 7 and day 14 for aRW treatment = 0.292, for comparison between day 7 and day 14 for aJ2 treatment = 1.38E-4. Total n of SGs quantified per treatment: aRW at 7days = 18, aRW at 14days = 19, aJ2 at 7days = 22, aJ2 at 14 days = 29. (i,j) Representative co-stain images for AR and FASN in SGs from

mice (n = 5 each) treated with aRW (i) and aJ2 (j), 14 days post treatment. (k) Quantification of the number of cells expressing AR in each SG, 7 and 14 days after treatment with aRW and aJ2. p-values: for comparison between day 7 and day 14 for aRW treatment = 0.273, for comparison between day 7 and day 14 for aJ2 treatment = 9.53E-09. Total n of SGs quantified per treatment: aRW at 7days = 12, aRW at 14days = 10, aJ2 at 7days = 18, aJ2 at 14 days = 23. Student's T-test used for statistical analysis. Error bars represent SEM. Scale bars are 25 μm.

Figure S1. Sebaceous ducts remain unaffected after Notch inhibition. (Related to Figure 1)

(a) Quantification of the percentage of SGs consisting of bursting sebocytes after each treatment at 7 days. p-values: aJ1 = 0.662, aJ2 = 0.782, aJ1J2 = 0.219. (b) Representative H&E images of SGs from mice (n = 5 each) treated with aRW, aJ1, aJ2 and aJ1J2, 7 days post treatment. Total n of SGs quantified per treatment: aRW = 66, aJ1 = 66, aJ2 = 68, aJ1J2 = 47. Student's T-test used for statistical analysis. Error bars represent SEM. Scale bars are 100 μm.

Figure S2. Notch is active in the sebaceous gland stem cells. (Related to Figure 2)

(a-c) Quantification of the location of N1ICD+ basal stem cells in SGs from mice (n = 5 each) treated with aRW (a), aJ1 (b) and aJ2 (c), 3 days post treatment. The SG was divided into five sections along the proximal-distal axis. The number of N1ICD+ basal stem cells in each section was divided by the total number of N1ICD+ basal stem cells in each SG. Total n of SGs quantified per treatment: aRW = 13, aJ1 = 15, aJ2 = 15. (d)

Quantification of what percentage of the total basal stem cells (N1ICD+ and N1ICD-) express both N1 ISH and J2 ISH. Total n of SGs quantified per treatment: aRW = 13, aJ1 = 15, aJ2 = 15. (e,f) Representative triple stain images for N1ICD, Notch1 and Jag2 mRNA in SGs from mice (n = 5 each) treated with (e) aRW and (f) aJ2, 3 days post treatment. (g) Quantification of the width of the IFE, 7 days after treatment with aRW, aJ1, aJ2 and aJ1J2. p-values: aJ1 = 0.528, aJ2 = 0.885, aJ1J2 = 0.840. Total n of SGs quantified per treatment: aRW = 26, aJ1 = 27, aJ2 = 27, aJ1J2 = 22. (h) Quantification of the width of the adipocyte layer, 7 days after treatment with aRW, aJ1, aJ2 and aJ1J2. p-values: aJ1 = 0.890, aJ2 = 0.948, aJ1J2 = 0.374. Total n of SGs quantified per treatment: aRW = 13, aJ1 = 13, aJ2 = 15, aJ1J2 = 15. (i,j) Representative H&E images of SGs from mice (n = 5 each) treated with aRW (i) and aJ2 (j), 7 days post treatment. Student's T-test used for statistical analysis. Error bars represent SEM. Scale bars are 100 µm.

Figure S3. Loss of Notch activity in the SG stem cells inhibits sebocyte differentiation. (Related to Figure 3)

(a) A representative co-stain image for N1ICD and FASN in an SG from mice (n = 5 each) treated with aJ1, 3 days post treatment. (b,c) Representative FASN staining in SGs from mice (n = 5 each) treated with aRW (b) and aJ2 (c), 3 days post treatment. (d) A representative adipophillin staining in an SG from mice (n = 5 each) treated with aJ1, 3 days post treatment. (e) A representative FASN staining in an SG from mice (n = 5 each) treated with aJ1, 3 days post treatment. (f,g) Representative FASN staining in SGs from mice (n = 5 each) treated with aRW (f) and aJ2 (g), 7 days post treatment. (h)

A representative adipophillin staining in an SG from mice (n = 5 each) treated with aJ1, 7 days post treatment. (i) A representative FASN staining in an SG from mice (n = 5 each) treated with aJ1, 7 days post treatment. (j) A representative adipophillin staining in an SG from mice (n = 5 each) treated with aJ1J2, 7 days post treatment. (i) A representative FASN staining in an SG from mice (n = 5 each) treated with aJ1J2, 7 days post treatment. Scale bars are 25 μm.

Figure S4. Notch activity in the SG stem cells is required to prevent unregulated progenitor proliferation. (Related to Figure 4)

(a,b) Representative co-stain images for Lrig1 and AR in SGs from mice (n = 5 each) treated with aRW (a) and aJ1 (b), 3 days post treatment. (c-e) Representative co-stain images for Lrig1 and AR in SGs from mice (n = 5 each) treated with aRW (c), aJ1 (d), and aJ1J2 (e), 7 days post treatment. (f,g) Representative co-stain images for Ki67 and FASN in SGs from mice (n = 5 each) treated with aRW (f) and aJ1 (g), 7 days post treatment. Scale bars are 25 μm.

Figure S5. The block in sebocyte differentiation is lifted upon recovery of Notch activity. (Related to Figure 5)

(a-c) Representative co-stain images for N1ICD and FASN in SGs from mice (n = 5 each) treated with aRW (a), aJ1 (b), and aJ1J2 (c), 7 days post treatment. (d) Quantification of the percentage of N1ICD+ cells in SGs from mice (n = 5 each) treated with aRW, aJ1, aJ2 and aJ1J2, 7 days post treatment. Percentage was calculated by dividing the number N1ICD+ cells by total number of basal-like cells in each SG. p-

values: aJ1 = 0.878, aJ2 = 3.42E-21, aJ1J2 = 5.60E-09. Total n of SGs quantified per treatment: aRW = 13, aJ1 = 13, aJ2 = 22, aJ1J2 = 13. (e-g) Representative adipophillin staining in SGs from mice (n = 5 each) treated with aRW (e), aJ1 (f), and aJ1J2 (g), 14 days post treatment. (h) Quantification of the number of cells expressing adipophilin in each SG, 14 days after treatment with aRW, aJ1, aJ2 and aJ1J2. p-values: aJ1 = 0.693, aJ2 = 3.40E-08, aJ1J2 = 0.003. Total n of SGs quantified per treatment: aRW = 19, aJ1 = 13, aJ2 = 29, aJ1J2 = 16. (i-k) Representative co-stain images for AR and FASN in SGs from mice (n = 5 each) treated with aRW (i), aJ1 (j), and a1J2 (k), 14 days post treatment. (l) Quantification of the number of cells expressing AR in each SG, 14 days after treatment with aRW, aJ1, aJ2 and aJ1J2. p-values: aJ1 = 0.248, aJ2 = 0.817, aJ1J2 = 0.032. Total n of SGs quantified per treatment: aRW = 10, aJ1 = 7, aJ2 = 23, aJ1J2 = 18.Student's T-test used for statistical analysis. Error bars represent SEM. Scale bars are 25 µm.

References

Ables JL, Breunig JJ, Eisch AJ, Rakic P. 2011. Not(ch) just development: Notch signalling in the adult brain. *Nat Rev Neurosci* **12**:269–283. doi:10.1038/nrn3024

Al-Zaid T, Vanderweil S, Zembowicz A, Lyle S. 2011. Sebaceous gland loss and inflammation in scarring alopecia: A potential role in pathogenesis. *J Am Acad Dermatol* **65**:597–603. doi:10.1016/j.jaad.2010.09.774

Andersen MS, Hannezo E, Ulyanchenko S, Estrach S, Antoku Y, Pisano S, Boonekamp KE, Sendrup S, Maimets M, Pedersen MT, Johansen JV, Clement DL, Feral CC, Simons BD, Jensen KB. 2019. Tracing the cellular dynamics of sebaceous gland development in normal and perturbed states. *Nat Cell Biol* **21**:924–932. doi:10.1038/s41556-019-0362-x

Belandia B, Powell SM, García-Pedrero JM, Walker MM, Bevan CL, Parker MG. 2005. Hey1, a Mediator of Notch Signaling, Is an Androgen Receptor Corepressor. *Mol Cell Biol* **25**:1425–1436. doi:10.1128/mcb.25.4.1425-1436.2005

Binczek E, Jenke B, Holz B, Günter RH, Thevis M, Stoffel W. 2007. Obesity resistance of the stearoyl-CoA desaturase-deficient (scd1 -/-) mouse results from disruption of the epidermal lipid barrier and adaptive thermoregulation. *bchm* **388**:405–418. doi:10.1515/bc.2007.046

Blanpain C, Lowry WE, Pasolli HA, Fuchs E. 2006. Canonical notch signaling functions as a commitment switch in the epidermal lineage. *Genes Dev* **20**:3022–3035. doi:10.1101/gad.1477606

Buitrago W, Joseph AK. 2008. Sebaceous carcinoma: the great masquerader. *Dermatol Ther* **21**:459–466. doi:10.1111/j.1529-8019.2008.00247.x

Cottle DL, Kretzschmar K, Schweiger PJ, Quist SR, Gollnick HP, Natsuga K, Aoyagi S, Watt FM. 2013. c-MYC-Induced Sebaceous Gland Differentiation Is Controlled by an Androgen Receptor/p53 Axis. *Cell Rep* **3**:427–441. doi:10.1016/j.celrep.2013.01.013

Estrach S, Ambler CA, Celso CLL, Hozumi K, Watt FM. 2006. Jagged 1 is a β-catenin target gene required for ectopic hair follicle formation in adult epidermis. *Development* **133**:4427–4438. doi:10.1242/dev.02644

Estrach S, Cordes R, Hozumi K, Gossler A, Watt FM. 2008. Role of the Notch Ligand Delta1 in Embryonic and Adult Mouse Epidermis. *J Investig Dermatol* **128**:825–832. doi:10.1038/sj.jid.5701113

Frances D, Niemann C. 2012. Stem cell dynamics in sebaceous gland morphogenesis in mouse skin. *Dev Biol* **363**:138–146. doi:10.1016/j.ydbio.2011.12.028

Jung Y, Tam J, Jalian HR, Anderson RR, Evans CL. 2015. Longitudinal, 3D In Vivo Imaging of Sebaceous Glands by Coherent Anti-Stokes Raman Scattering Microscopy: Normal Function and Response to Cryotherapy. *J Investig Dermatol* **135**:39–44. doi:10.1038/jid.2014.293

Kamińska A, Pardyak L, Marek S, Wróbel K, Kotula-Balak M, Bilińska B, Hejmej A. 2020. Notch signaling regulates nuclear androgen receptor AR and membrane androgen receptor ZIP9 in mouse Sertoli cells. *Andrology* **8**:457–472. doi:10.1111/andr.12691

Karnik P, Tekeste Z, McCormick TS, Gilliam AC, Price VH, Cooper KD, Mirmirani P. 2009. Hair Follicle Stem Cell-Specific PPARγ Deletion Causes Scarring Alopecia. *J Investig Dermatol* **129**:1243–1257. doi:10.1038/jid.2008.369

Kretzschmar K, Cottle DL, Donati G, Chiang M-F, Quist SR, Gollnick HP, Natsuga K, Lin K-I, Watt FM. 2014. BLIMP1 Is Required for Postnatal Epidermal Homeostasis but Does Not Define a Sebaceous Gland Progenitor under Steady-State Conditions. *Stem Cell Rep* **3**:620–633. doi:10.1016/j.stemcr.2014.08.007

Lafkas D, Shelton A, Chiu C, Boenig G de L, Chen Y, Stawicki SS, Siltanen C, Reichelt M, Zhou M, Wu X, Eastham-Anderson J, Moore H, Roose-Girma M, Chinn Y, Hang JQ, Warming S, Egen J, Lee WP, Austin C, Wu Y, Payandeh J, Lowe JB, Siebel CW. 2015. Therapeutic antibodies reveal Notch control of transdifferentiation in the adult lung. *Nature* **528**:127–131. doi:10.1038/nature15715

Lavery DN, Villaronga MA, Walker MM, Patel A, Belandia B, Bevan CL. 2011. Repression of Androgen Receptor Activity by HEYL, a Third Member of the Hairy/Enhancer-of-split-related Family of Notch Effectors*. *J Biol Chem* **286**:17796–17808. doi:10.1074/jbc.m110.198655

Lovászi M, Szegedi A, Zouboulis CC, Törőcsik D. 2017. Sebaceous-immunobiology is orchestrated by sebum lipids. *Derm-Endocrinol* **9**:00–00. doi:10.1080/19381980.2017.1375636

Mosteiro L, Nguyen TTT, Hankeova S, Alvarez-Sierra D, Reichelt M, Vandriel SM, Lai Z, Choudhury FK, Sangaraju D, Kamath BM, Scherl A, Pujol-Borrell R, Piskol R, Siebel CW. 2023. Notch signaling in thyrocytes is essential for adult thyroid function and mammalian homeostasis. *Nat Metab* **5**:2094–2110. doi:10.1038/s42255-023-00937-1

Nelson BR, Hamlet KR, Gillard M, Railan D, Johnson TM. 1995. Sebaceous carcinoma. *J Am Acad Dermatol* **33**:1–15. doi:10.1016/0190-9622(95)90001-2

Niemann C, Horsley V. 2012. Development and homeostasis of the sebaceous gland. *Semin Cell Dev Biol* **23**:928–936. doi:10.1016/j.semcdb.2012.08.010

Ostler DA, Prieto VG, Reed JA, Deavers MT, Lazar AJ, Ivan D. 2010. Adipophilin expression in sebaceous tumors and other cutaneous lesions with clear cell histology: an immunohistochemical study of 117 cases. *Mod Pathol* **23**:567–573. doi:10.1038/modpathol.2010.1

Page ME, Lombard P, Ng F, Göttgens B, Jensen KB. 2013. The Epidermis Comprises Autonomous Compartments Maintained by Distinct Stem Cell Populations. *Cell Stem Cell* **13**:471–482. doi:10.1016/j.stem.2013.07.010

Pan Y, Lin M-H, Tian X, Cheng H-T, Gridley T, Shen J, Kopan R. 2004. γ-Secretase Functions through Notch Signaling to Maintain Skin Appendages but Is Not Required for Their Patterning or Initial Morphogenesis. *Dev Cell* **7**:731–743. doi:10.1016/j.devcel.2004.09.014

Rittié L, Tejasvi T, Harms PW, Xing X, Nair RP, Gudjonsson JE, Swindell WR, Elder JT. 2016. Sebaceous Gland Atrophy in Psoriasis: An Explanation for Psoriatic Alopecia? *J Investig Dermatol* **136**:1792–1800. doi:10.1016/j.jid.2016.05.113

Sato C, Zhao G, Ilagan MXG. 2012. An Overview of Notch Signaling in Adult Tissue Renewal and Maintenance. *Curr Alzheimer Res* **9**:227–240. doi:10.2174/156720512799361600

Schirra F, Suzuki T, Richards SM, Jensen RV, Liu M, Lombardi MJ, Rowley P, Treister NS, Sullivan DA. 2005. Androgen Control of Gene Expression in the Mouse Meibomian Gland. *Investig Opthalmology Vis Sci* **46**:3666. doi:10.1167/iovs.05-0426

Schneider MR, Paus R. 2010. Sebocytes, multifaceted epithelial cells: Lipid production and holocrine secretion. *Int J Biochem Cell Biol* **42**:181–185. doi:10.1016/j.biocel.2009.11.017

Seiffert K, Seltmann H, Fritsch M, Zouboulis C. 2007. Inhibition of 5α-Reductase Activity in SZ95 Sebocytes and HaCaT Keratinocytes In Vitro. *Horm Metab Res* **39**:141–148. doi:10.1055/s-2007-961814

Shi VY, Leo M, Hassoun L, Chahal DS, Maibach HI, Sivamani RK. 2015. Role of sebaceous glands in inflammatory dermatoses. *J Am Acad Dermatol* **73**:856–863. doi:10.1016/j.jaad.2015.08.015

Siebel C, Lendahl U. 2017. Notch Signaling in Development, Tissue Homeostasis, and Disease. *Physiol Rev* **97**:1235–1294. doi:10.1152/physrev.00005.2017

Smith KR, Thiboutot DM. 2008. Thematic review series: Skin Lipids. Sebaceous gland lipids: friend or foe? *J Lipid Res* **49**:271–281. doi:10.1194/jlr.r700015-jlr200

Stenn KS, Sundberg JP, Sperling LC. 1999. Hair Follicle Biology, the Sebaceous Gland, and Scarring Alopecias. *Arch Dermatol* **135**:973–974. doi:10.1001/archderm.135.8.973

Tran IT, Sandy AR, Carulli AJ, Ebens C, Chung J, Shan GT, Radojcic V, Friedman A, Gridley T, Shelton A, Reddy P, Samuelson LC, Yan M, Siebel CW, Maillard I. 2013. Blockade of individual Notch ligands and receptors controls graft-versus-host disease. *J Clin Investig* **123**:1590–1604. doi:10.1172/jci65477

Veniaminova NA, Grachtchouk M, Doane OJ, Peterson JK, Quigley DA, Lull MV, Pyrozhenko DV, Nair RR, Patrick MT, Balmain A, Dlugosz AA, Tsoi LC, Wong SY. 2019. Niche-Specific Factors Dynamically Regulate Sebaceous Gland Stem Cells in the Skin. *Dev Cell* **51**:326-340.e4. doi:10.1016/j.devcel.2019.08.015

Veniaminova NA, Jia YY, Hartigan AM, Huyge TJ, Tsai S-Y, Grachtchouk M, Nakagawa S, Dlugosz AA, Atwood SX, Wong SY. 2023. Distinct mechanisms for sebaceous

gland self-renewal and regeneration provide durability in response to injury. *Cell Rep* **42**:113121. doi:10.1016/j.celrep.2023.113121

Watt FM, Estrach S, Ambler CA. 2008. Epidermal Notch signalling: differentiation, cancer and adhesion. *Curr Opin Cell Biol* **20**:171–179. doi:10.1016/j.ceb.2008.01.010

Wilson A, Radtke F. 2006. Multiple functions of Notch signaling in self-renewing organs and cancer. *FEBS Lett* **580**:2860–2868. doi:10.1016/j.febslet.2006.03.024

Wu Y, Cain-Hom C, Choy L, Hagenbeek TJ, Leon GP de, Chen Y, Finkle D, Venook R, Wu X, Ridgway J, Schahin-Reed D, Dow GJ, Shelton A, Stawicki S, Watts RJ, Zhang J, Choy R, Howard P, Kadyk L, Yan M, Zha J, Callahan CA, Hymowitz SG, Siebel CW. 2010. Therapeutic antibody targeting of individual Notch receptors. *Nature* **464**:1052–1057. doi:10.1038/nature08878

Yu J, Siebel CW, Schilling L, Canalis E. 2020. An antibody to Notch3 reverses the skeletal phenotype of lateral meningocele syndrome in male mice. *J Cell Physiol* **235**:210–220. doi:10.1002/jcp.28960

Figure 1. Jag2 is the dominant ligand involved in regulating sebocyte differentiation.

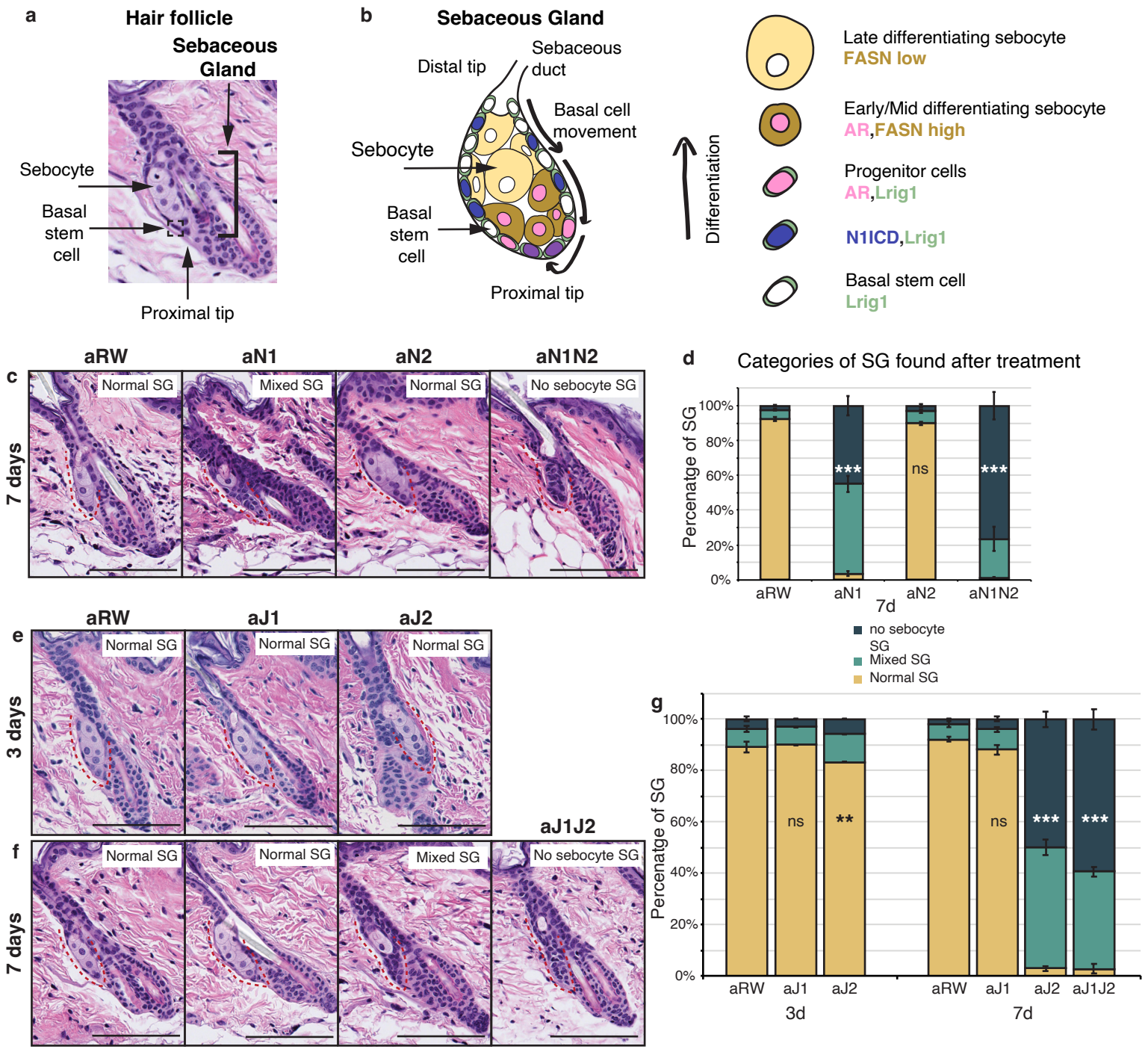

Figure 2. Notch is active in the sebaceous gland stem cells.

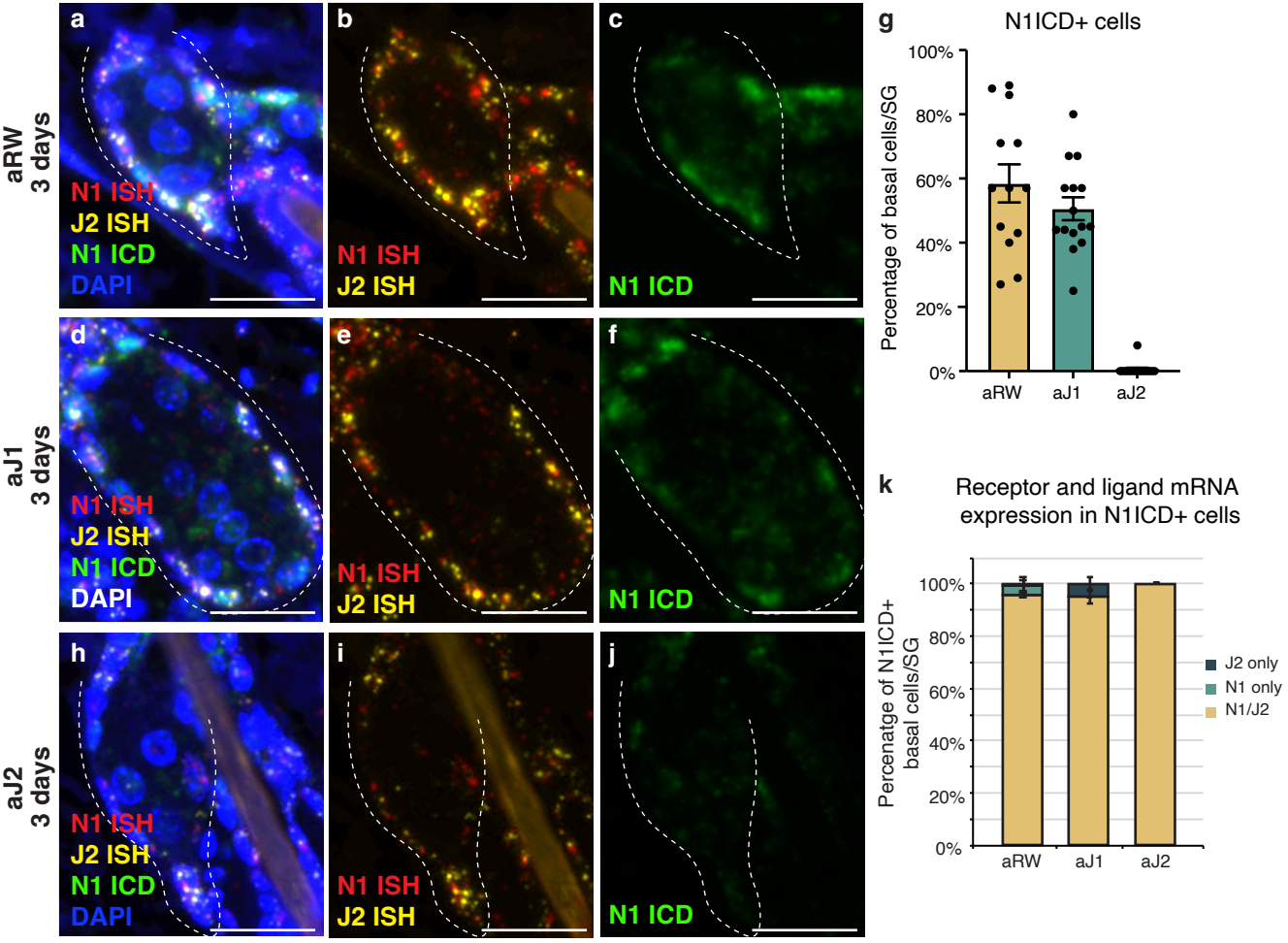

Figure 3. Loss of Notch activity in the SG stem cells inhibits sebocyte differentiation.

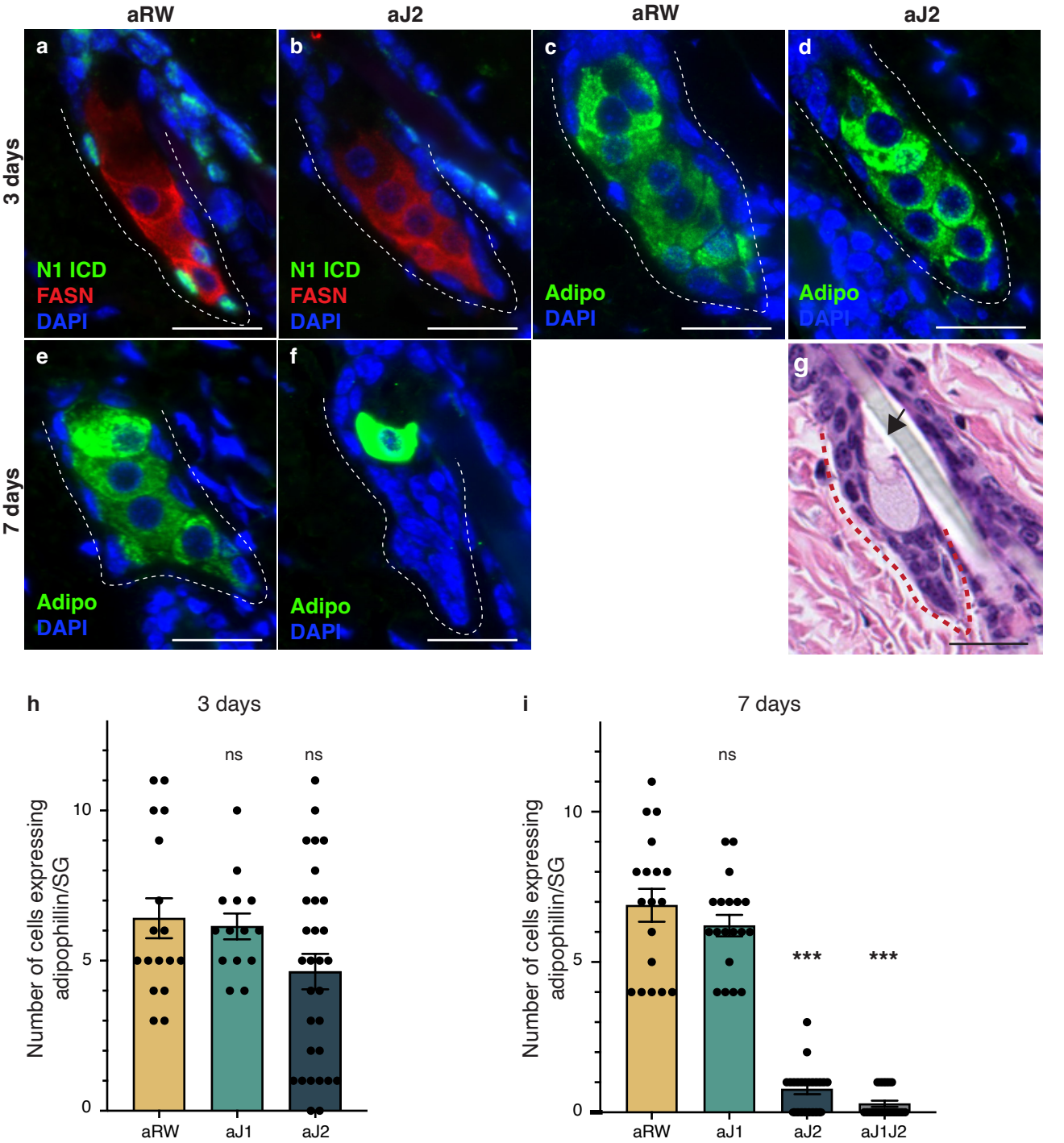

Figure 4. Notch activity in the SG stem cells is required to prevent unregulated progenitor proliferation.

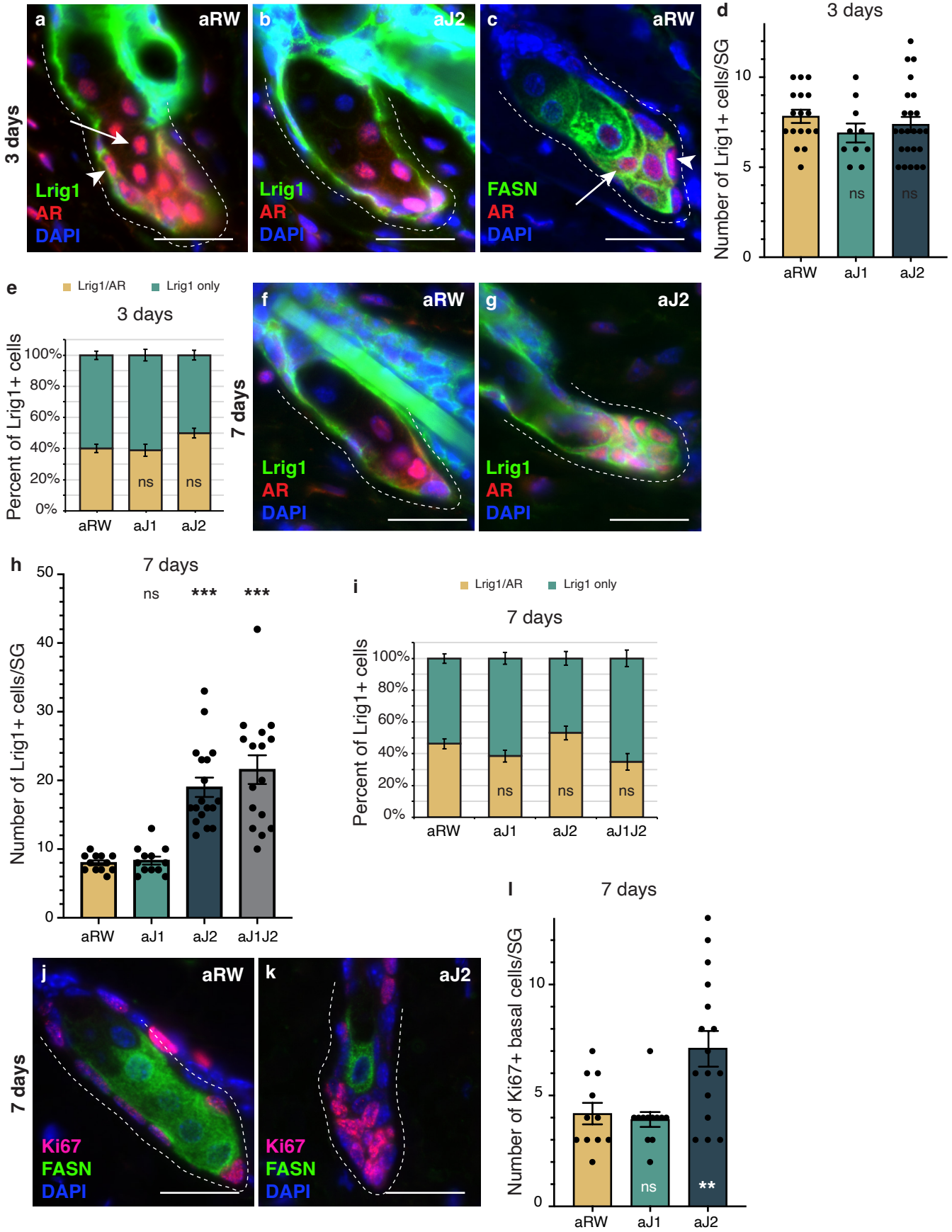
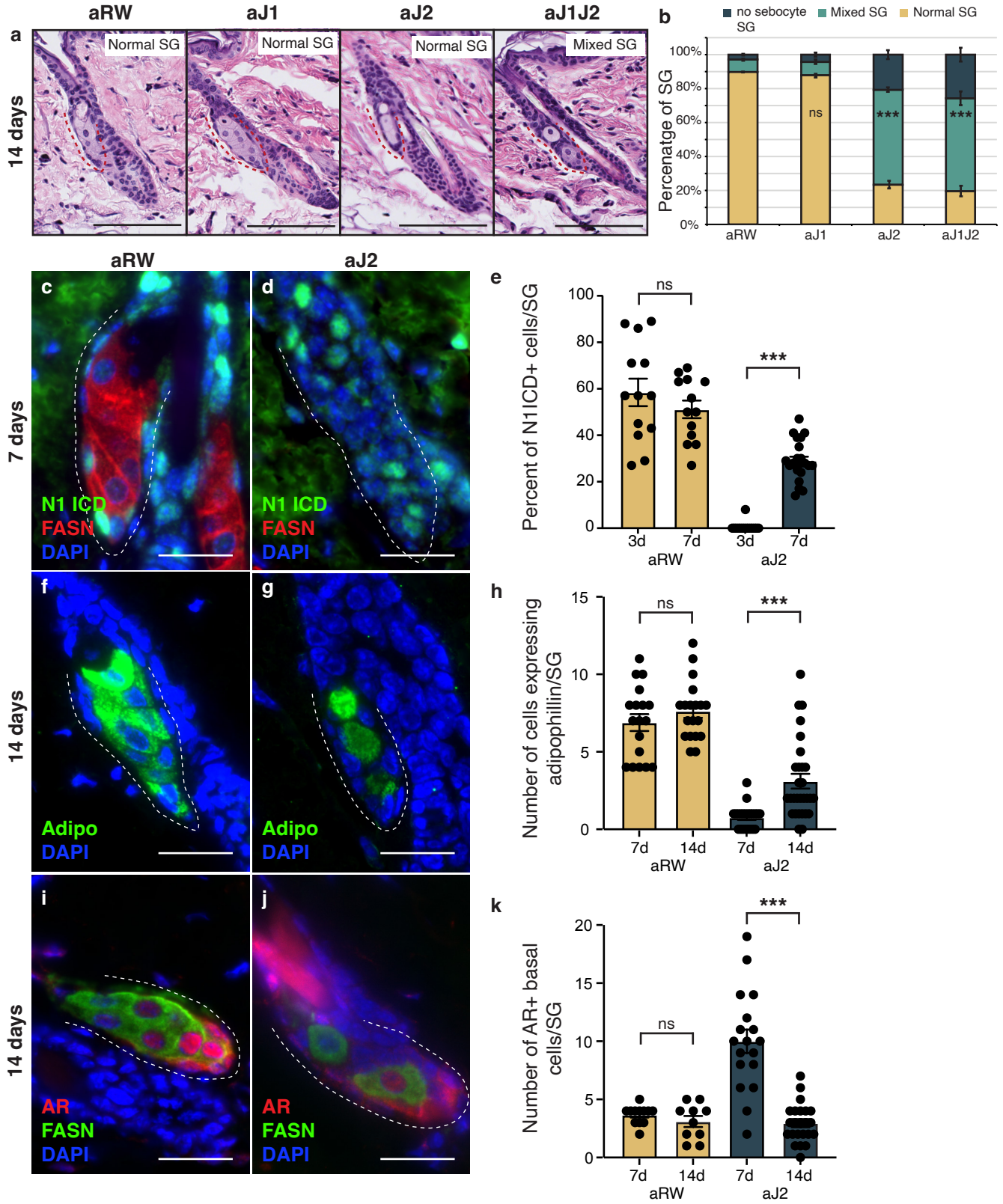
Figure 5. The block in sebocyte differentiation is lifted upon recovery of Notch activity.